Spectroscopic investigation of the electronic structure of the hole-doped one-dimensional cuprates Ca_2CuO_3 and Sr_2CuO_3

K. Maiti* and D. D. Sarma†
Solid State and Structural Chemistry Unit, Indian Institute of Science, Bangalore 560 012, India
(Received 5 May 2001; revised manuscript received 14 August 2001; published 26 April 2002)

We investigate the effect of hole doping in the electronic structure of covalent insulators, Ca_2CuO_3 and Sr_2CuO_3 by means of photoelectron spectroscopy. The changes in the core level, valence-band and conduction-band spectra indicate a doping-induced small modification in the interaction parameters. The doped holes are found to be localized primarily at the apical oxygen sites.

DOI: 10.1103/PhysRevB.65.174517 PACS number(s): 79.60.Bm, 71.27.+a, 74.72.Jt

I. INTRODUCTION

Abundance of superconductivity in hole-doped two-dimensional divalent cuprates has opened up an interesting field of research. It is believed that the electronic structure of Cu-O planes plays the key role in high-temperature superconductivity.[1,2] While it is challenging to understand the microscopic origin of such an effect in these systems, the low-dimensional cuprates also provide a good testing ground to verify rigorous solutions of theoretical models, often inaccessible for systems in higher dimensions. One-dimensional systems have drawn further attention due to their diverse physical properties such as a van Hove singularity on the spin Fermi surface,[3] spin-charge separation,[4,5] interesting spin dynamics,[6,7] covalent insulating behavior,[8,9] associated with the low dimensionality. Interestingly, it has been reported that oxygen excess in Sr_2CuO_3, a hole-doped system prepared under high pressure in an oxidizing atmosphere, leads to superconductivity ($T_c = 70$ K for $\delta = 0.1$ in $Sr_2CuO_{3+\delta}$), along with a change in the structure of the parent compound.[10] However, hole doping *via* monovalent Na substitution in $M_{2-x}Na_xCuO_3$ (M = Sr/Ca) barely changes the transport properties.[11]

In order to investigate the role of doped holes in these Na substituted one-dimensional cuprates, we study the electronic structure of $M_{2-x}Na_xCuO_3$ (M = Sr/Ca) by means of photoelectron spectroscopies. The structure of Sr_2CuO_3 and Ca_2CuO_3 is K_2NiF_4 derived.[12] The CuO_4 polyhedra are linked by sharing corners only along one crystal axis b with a Cu-O-Cu angle of 180°. The CuO_4 units are almost perfect squares in Sr_2CuO_3, but distorted in Ca_2CuO_3 with a smaller Cu-O distance along the chain axis.[13] Such a distortion in the chains arises due to the smaller ionic radius of Ca^{2+} (1.06 Å) compared to that of Sr^{2+} (1.21 Å).[14] The significantly larger separation between the CuO chains and the absence of oxygen along the directions perpendicular to the chain axis compared to that along the chains lead to a negligibly small interchain coupling; this is manifested by their low three-dimensional antiferromagnetic ordering temperatures (~5 K). Thus, the electronic properties of these compounds are essentially governed by the one-dimensional Cu-O chains.

Transport measurements on these systems indicate an activation energy of about 0.18 eV for the thermal excitation of charge carriers in both compounds,[13] while optical measurements suggest considerably larger gaps in Ca_2CuO_3 (~1.75 eV) (Ref. 15) and in Sr_2CuO_3 (~1.5 eV).[8,9] The estimates of various electronic interaction strengths from the analysis of the photoemission spectra in terms of model many-body calculations, suggest that the charge-transfer energy Δ is in general, smaller in these compounds compared to other cuprates, such as La_2CuO_4 (two-dimensional) and CuO (three-dimensional), though all other interaction parameters are essentially similar.[8,9] The small Δ was attributed to the reduced Madelung potential in these systems similar to the trend with dimensionality observed in nickelates.[16] Such a small Δ in one-dimensional cuprates leads to an unusual electronic structure with the empty upper Hubbard band within the oxygen $2p$ bandwidth. This is particularly so for Sr_2CuO_3 that has an even lower Δ than Ca_2CuO_3. The insulating behavior despite the small Δ establishes these systems as examples of covalent insulators.[17,18]

Doping of Sr_2CuO_3 with Na shrinks the CuO_4 units with a smaller Cu-O bond length, thereby reducing the corresponding lattice constants, while the lattice constant perpendicular to the CuO_4 units is found to increase with doping.[11] The basic structure type does not change in the whole composition range. Magnetic susceptibility measurements exhibit weak signals, suggesting the presence of strong intrachain antiferromagnetic interactions in the doped compounds. A low-spin configuration of Cu^{3+} is observed in $NaSrCuO_3$.[19]

Doped holes reduce the resistivity considerably, though no signature of a metallic phase is observed in the entire composition range. The charge transport in the doped compounds is primarily driven by the hopping of small polarons.[19] Similarly, Na substitution in Ca_2CuO_3 also decreases the resistivity with negligible effect on magnetic properties.[20]

In this study, we investigate the electronic structure of $Sr_{2-x}Na_xCuO_3$ and $Ca_{2-x}Na_xCuO_3$ by means of photoemission and inverse photoemission spectroscopies. The results suggest a localization of the doped holes at the apical oxygen sites. While the spectral functions for the Cu $2p$ core level and valence band suggest a small modification of the electronic interaction parameters with doping, the conduction band exhibits unusual spectral changes. Specifically, the redistribution in spectral weights in $Sr_{2-x}Na_xCuO_3$ exhibits a spectral-weight transfer in the conduction band away from the Fermi level in contrast to the usual spectral-weight trans-

fer towards the Fermi level observed in the strongly correlated systems.[21–23]

II. EXPERIMENT

Sr_2CuO_3 and Ca_2CuO_3 were prepared by solid-state reactions in air at 900 °C for 24 h, starting with stoichiometric amounts of $SrCO_3$, CuO and $CaCO_3$, CuO, respectively. The powders were further heated at 1000 °C and 950 °C for Sr_2CuO_3 and Ca_2CuO_3, respectively, with several intermittent grindings. $Ca_{1.8}Na_{0.2}CuO_3$ was prepared following the preparation procedure and conditions of Ca_2CuO_3 using Na_2CO_3 in addition to $CaCO_3$ and CuO. Since sodium is a highly reactive material and volatile at higher temperatures, all the heat treatments were carried out for shorter durations keeping the ingredients in a platinum crucible. The crystal structure was monitored at each heating interval to minimize the number of heat treatments required, in order to reduce the Na loss. However, a well sintered $Sr_{1.8}Na_{0.2}CuO_3$ could not be synthesized by this procedure. Thus, we followed the sol-gel route to prepare this sample. This procedure helps in minimizing the number of heat treatments by providing a better mixture of the ingredient materials in the beginning. The dried gel was treated successively at 450 °C, 600 °C, 800 °C, and 1000 °C for 24 h, 30 h, 24 h, and 18 h, respectively, with several intermittent grindings. The final treatments were always performed on a pellet form and the samples were inserted into the analysis chamber immediately after the final treatment, in order to avoid the degradation of the sample by exposure to the atmosphere. All the samples were characterized by x-ray powder-diffraction (XRD) patterns obtained from a JEOL-8P x-ray diffractometer. The XRD patterns suggest the same crystal structure type for all the compositions in each case. The samples were found to have single phase and the lattice constants obtained for these XRD patterns agree well with those reported in the literature.[11] While the doping of hole states was confirmed by the oxygen stoichiometery measurements, a small loss of oxygen was observed in the doped compositions compared to the parent compounds.

Electron spectroscopic measurements were carried out in a combined XPS-UPS-BIS spectrometer from VSW Instruments Ltd., UK. The resolution for the ultraviolet photoemission (UP) and x-ray photoemission (XP) spectroscopic measurements were 0.1 eV and 0.8 eV, respectively. These techniques probe the occupied part of the electronic structure. The unoccupied part was probed by bremsstrahlung isochromat (BI) spectroscopy with a total resolution of 0.8 eV at an energy of 1486.6 eV. The samples were scraped *in situ* with an alumina file to obtain clean and reproducible surfaces. The experiments were performed at liquid-nitrogen temperature to reduce the surface degradation and the cleanliness was monitored by the intensity of the higher binding-energy features of the O 1*s* peak and the integrated C 1*s* signal. After scraping, the C 1*s* photoemission signal could not be observed in any of the samples. The intensities corresponding to the oxygen impurity related features in Ca compounds were negligible; however, a small intensity at about 1.5 eV higher binding energy relative to the main O 1*s* signal could not be avoided in Sr compounds even after several scrapings. The reproducibility of all the spectra was confirmed after each scraping of the same sample as well as different samples with same compositions. No charging effect was observed in the doped compositions and in Sr_2CuO_3. A small constant shift in energy was observed in the BI spectrum of Ca_2CuO_3. Thus, we have shifted the corresponding spectrum, so that it is consistent with the optical measurements by Tokura *et al.* (Ref. 15) and also consistent with the spectrum of the doped sample.

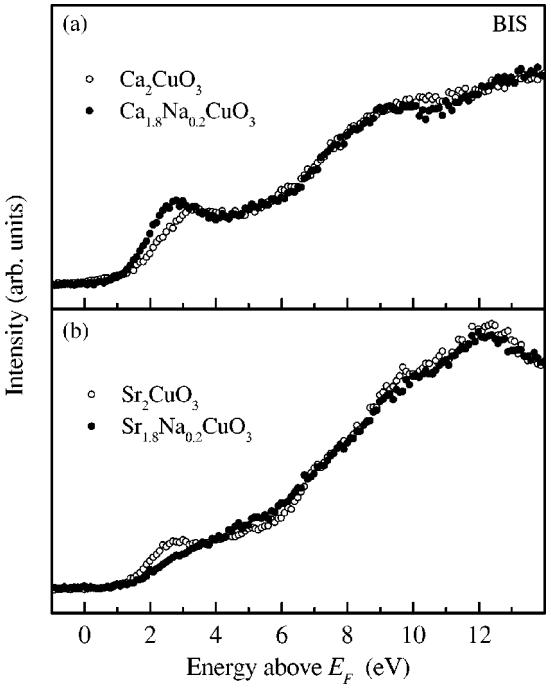

FIG. 1. BI spectra of (a) $Ca_{2-x}Na_xCuO_3$ and (b) $Sr_{2-x}Na_xCuO_3$ for $x=0.0$ (open circles) and 0.2 (solid circles).

III. RESULTS AND DISCUSSION

We show the BI spectra corresponding to the conduction band in Fig. 1. The spectra corresponding to Ca_2CuO_3 and Sr_2CuO_3 are represented by open circles in Figs. 1(a) and 1(b), respectively. The features related to Sr and Ca appear beyond 6 eV above the Fermi level. Since the oxygen *p* bands in these covalent insulators appear above the Cu *d* bands, the conduction band will be dominated by the oxygen *p* contributions. The broad peak at about 3 eV above E_F is essentially due to the transitions of the electrons to the O *p*–Cu *d* related levels. The absence of spectral intensity at E_F is consistent with the observed insulating properties and the large energy band gap in these systems.

The electronic configuration of Cu in the ground state of both Sr_2CuO_3 and Ca_2CuO_3 corresponds to $3d^9$. Hence, there is only one hole in the conduction band. Thus, the changes in the electronic structure due to hole doping are expected to be most pronounced in the conduction-band region. We overlap the BI spectra of doped compounds (solid circles) over the undoped ones to illustrate the changes in the conduction band on doping. The spectral features are normalized beyond 20 eV above E_F, a region contributed by

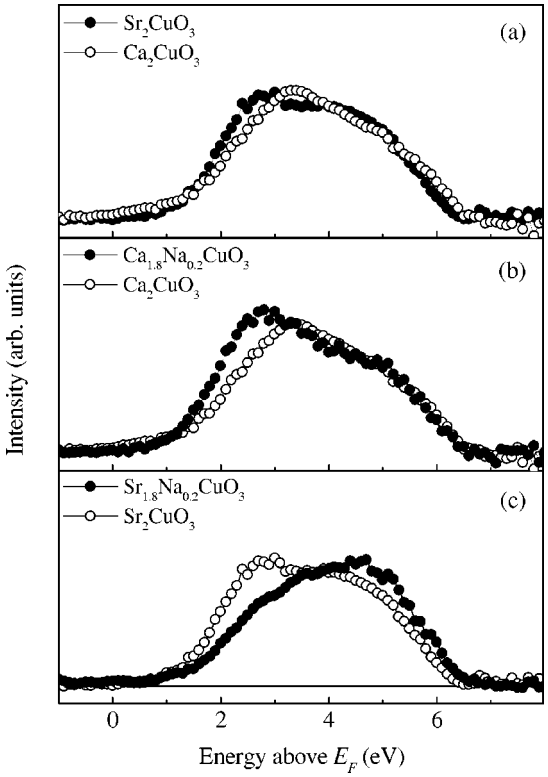

FIG. 2. BI spectra of (a) Ca_2CuO_3 (open circles) and Sr_2CuO_3 (solid circles), and (b) $Ca_{2-x}Na_xCuO_3$ and (c) $Sr_{2-x}Na_xCuO_3$ for $x=0.0$ (open circles) and 0.2 (solid circles). These spectral functions are obtained after the subtraction of the features appearing beyond 6 eV above E_F simulated by a combination of Lorentzians and Gaussians.

high-energy continuum states. The spectral shapes for doped and undoped compounds are found to be very similar above 6 eV with a small change in intensity of the higher-energy features due to the reduction in the Ca/Sr content in the respective compounds relative to the undoped ones. The hole doping does not introduce any intensity at the Fermi level in these compounds, in agreement with the insulating character of the doped samples. However, the low-energy features exhibit substantial spectral modifications on doping. There is an increase in intensity around 2.8 eV above E_F as a function of doping in Ca_2CuO_3. On the other hand, the intensity of the 2.8-eV feature is reduced in the doped Sr_2CuO_3, with an enhancement around 5 eV, evidencing a transfer of spectral weight to a higher-energy region induced by hole doping.

In order to illustrate the changes in the spectra better, we simulate the features appearing beyond 6 eV above E_F by a combination of Lorentzians and Gaussians and subtract the simulated spectra from the experimental BI spectra of all the compounds. The subtracted spectra are shown in Fig. 2. First we compare the spectra of Ca_2CuO_3 and Sr_2CuO_3 in Fig. 2(a). The sharp features at lower energies are dominated by the Cu $3d$-symmetry-adapted oxygen $2p$ states.[24] It is clear that the feature around 2.8 eV above E_F is more intense in Sr_2CuO_3 than that in Ca_2CuO_3. In the latter, the strongest feature appears at about 3.4 eV along with a shoulder at 2.8 eV. Following the oxygen *K*-edge x-ray-absorption measurements and analysis,[25] the features around 2.8 eV and 3.4 eV above E_F can be attributed to oxygen $2p$ states arising primarily from the apical oxygens of the CuO_4 networks and the oxygens in the chain axis admixed with the Cu $3d_{x^2-y^2}$ states. Such different energies for the oxygen levels are due to the difference in Madelung potentials of these oxygens arising from the different number of nearest neighbors.[26,27] Since the CuO_4 network is almost perfectly square in Sr_2CuO_3 and is slightly compressed along the chain direction in Ca_2CuO_3, the increased intensity of the higher-energy feature in Ca_2CuO_3 may be attributed to the subtle changes in the hopping interaction strength due to the distortion of the CuO_4 network in Ca_2CuO_3.

The spectral features corresponding to doped and undoped compounds are overlapped in Figs. 2(b) and 2(c). No significant change in the conduction-band edge could be observed in the figure. The doping in Ca_2CuO_3 introduces a large increase in intensity at about 2.8 eV. It has been observed that the higher-dimensional cuprates exhibit an anomalous spectral-weight transfer to the Fermi level as a function of doping, leading to an insulator-to-metal transition.[21–23] Some of these systems were found to be high-temperature superconductors for certain compositions. The nickelates in one dimension,[28] as well as in higher dimensions,[29] also exhibit anomalous spectral-weight transfer similar to the higher-dimensional cuprates. Such spectral-weight transfer with doping a Mott insulator is well understood[30] within various theoretical models. Instead, in Ca_2CuO_3, the spectral weight related to the $2p$ states of the apical oxygens increases substantially with virtually no change at higher energies. This suggests that the doped holes are localized primarily at the apical oxygen sites in this system. The spectral changes in Sr_2CuO_3 appears to be significantly different and unusual. It appears that the intensity of the features close to E_F reduces, with an overall increase in intensity at higher energies. Such a doping-induced change has not been observed in any other system so far.

We now turn to the question of doping-induced changes in the valence-band spectra. The He I (UP) and XP valence band spectra of all the compounds are shown in Fig. 3. The spectra are normalized by the spectral intensity at about 5-eV binding energy. The strongest spectral intensity, around 4-eV binding energy in the XP spectrum of Ca_2CuO_3 [open circles in Fig. 3(a)], represents transitions from the nonbonding Cu $3d$ states with a_{1g} symmetry.[9] The spectral intensity around 3.5-eV binding energy becomes maximum in the UP spectrum and thus, suggests a large oxygen $2p$ character of this feature. The bonding features appear at higher binding energies. The spectra of Sr_2CuO_3 also exhibit similar spectral distributions. The large intensity around 4-eV binding energy in the XP spectrum in Fig. 3(b) reduces rapidly in the UP spectrum, with a significant increase in intensity around 2.8-eV binding energy. These modifications in intensity suggest the feature around 4 eV to be the nonbonding Cu $3d_{z^2}$ states with a_{1g} symmetry, while the features with dominant O $2p$ character appear around 2.8-eV binding energy. This unusual presence of the oxygen *p* related bands above the Cu *d* bands, in contrast to almost all other transition-metal oxides, was attributed to the small charge-transfer energy in

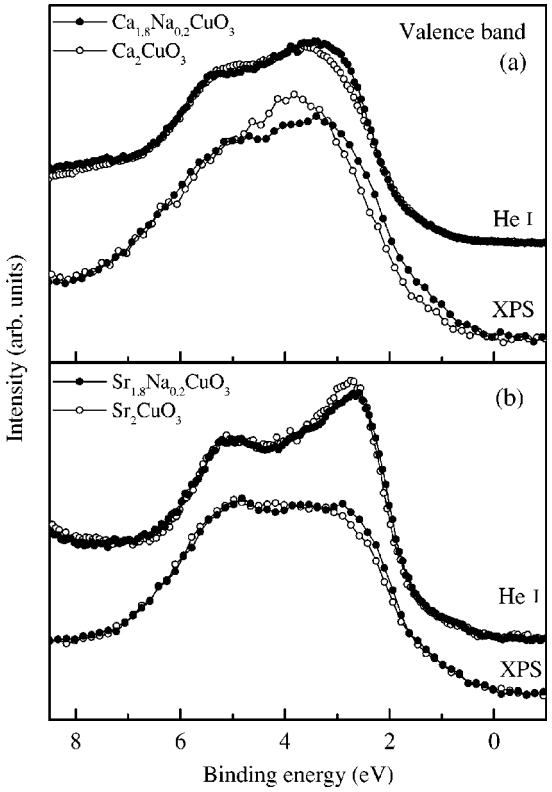

FIG. 3. Valence-band spectra of (a) $Ca_{2-x}Na_xCuO_3$ and (b) $Sr_{2-x}Na_xCuO_3$ for $x=0.0$ (open circles) and 0.2 (solid circles) for the He I and XPS (1256.6 eV) photon energies.

these systems, suggesting a correlated covalent insulating state.[9]

The hole doping introduces significant modifications in the spectral shape. In the case of $Ca_{2-x}Na_xCuO_3$, the spectra for $x=0.0$ and 0.2 are overlapped in Fig. 3(a). The spectral features beyond 4.5 eV are found to remain almost unchanged in both cases (He I and XP spectra), while there are modifications in the spectral intensities at lower binding energies. In the XP spectra, the intensity of the nonbonding Cu $3d_{z^2}$ states at about 4 eV reduces, with an increase in intensity at the leading edge, peaking at about 3.2-eV binding energy. Since the intensity due to the oxygen $2p$ states is not significant at this high electron kinetic energies,[31] the observed spectral change suggests lower binding energy of the nonbonding Cu $3d_{z^2}$ states at the doped sites. With the decrease in photon energy, the spectral intensity exhibits a maximum at about 2.8-eV binding energy. This variation in spectral intensities with photon energy and comparison with the consequent changes in the photoemission cross sections of the O $2p$ and Cu $3d$ related states suggest that the feature around 2.8 eV has a large oxygen $2p$ character. It is evident that the intensity around 2.8-eV binding energy in the He I spectrum of the doped compound is larger compared to that in the undoped compound. Such a spectral change is in contrast to the expected decrease in the electronic population in the valence band due to hole doping. No spectral intensity could be observed at the Fermi level, indicating the insulating nature of the system and is consistent with the observed transport properties.

The doping-induced modifications in the valence band of Sr_2CuO_3 are shown in Fig. 3(b). The spectral features are represented in the same way as in the previous case. The changes in the intensity of the spectral signatures in the doped composition compared to the parent one are considerably less pronounced in this case than in Fig. 3(a). The spectral features at higher binding energies remain unchanged with doping. The nonbonding Cu $3d$ levels exhibit a small shift in the XP spectra towards E_F, appearing as an overall enhancement in intensity at about 3-eV binding energy. Interestingly, the intensity around 2.8 eV is found to diminish with He I excitation for the doped sample. While there is a substantial increase in spectral weights in this energy region due to the shift of the nonbonding Cu d states, the overall decrease of the O $2p$ states with doping suggests dominant O $2p$ character of the doped holes in these systems. This observation is consistent with the conduction-band spectra shown in Fig. 1 and Fig. 2, and thus, confirms the O $2p$ character of the doped holes. As for $Ca_{2-x}Na_xCuO_3$, in this case also no intensity could be observed at the Fermi level indicating an insulating nature of this system.

The electronic configuration of the Cu^{2+} in these compounds is $d_{z^2}^2 d_{x^2-y^2}^1$, arising from the D_{4h} symmetry-induced splitting of the e_g level. Thus, the $d_{x^2-y^2}$ band with b_{1g} symmetry is half filled. Doping with holes will remove one electron at each doped site. The changes in the intensity of the bands corresponding to the apical oxygens, as observed in the conduction- and valence-band spectra, suggest that the ground-state configuration close to the doped sites is $d_{z^2}^2 d_{x^2-y^2}^1 \underline{L}$, with the ligand hole at the apical oxygen site. This ligand hole couples antiferromagnetically with the $3d$ hole. Thus, the ground state at the doped site is a singlet state and is consistent with the observation of low-spin configuration in the magnetic measurements in these systems.[19]

In disordered localized systems, the conduction band has been observed to resemble the sum of the contributions from the doped and undoped sites.[32–35] Thus, the conduction and valence bands in these systems are expected to be a composition-weighted sum of the contributions from the doped and undoped sites. While this may explain the situation in $Ca_{2-x}Na_xCuO_3$, the spectral modification in the conduction band of $Sr_{2-x}Na_xCuO_3$ cannot be explained within this framework.

It is important to note here that the smaller ionic radius of Na^{1+} ($\sim$1.12 Å) compared to that of Sr^{2+} ($\sim$1.21 Å) introduces a distortion in the CuO_4 network, reducing the bond lengths primarily along the chain direction b. The increased valency of Cu arising from monovalent Na substitution will further reduce the bond length due to the increased Coulombic attractions and the reduced radius of Cu^{3+} in comparison to Cu^{2+}.[11] This has been demonstrated schematically in Fig. 4. In the figure, we show the overlap of the Cu $3d_{x^2-y^2}$ orbitals and oxygen $2p$ orbitals. The apical oxygens and the oxygens on the chain axis are denoted by O(1) and O(2), respectively. The hopping interaction strength, t ($=\langle \psi_p | H | \psi_d \rangle$; H is the Hamiltonian of the system) be-

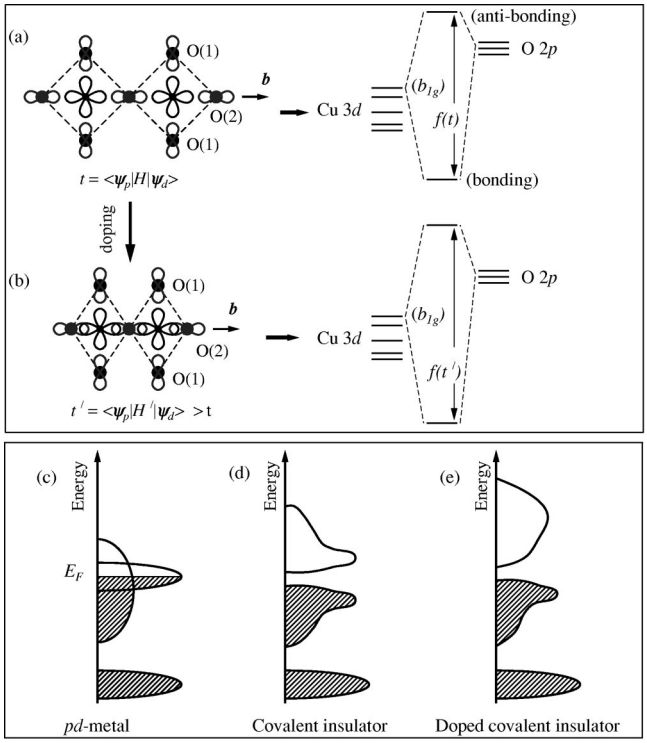

FIG. 4. (a) The Cu-O chains with almost perfectly square CuO_4 units in Sr_2CuO_3 and the corresponding energy-level diagram only for the bonding and antibonding states with b_{1g} symmetry. The antibonding states shown here contribute in the valence and conduction bands. (b) Heterovalent substitution leads to a distortion of the CuO_4 units along the chain direction, *b* and corresponding energy-level diagram. O(1) and O(2) are the oxygens at the apical sites and on the chain axis represented by large spheres and the small spheres refer to Cu. The schematics of the energy-band schemes for (c) *pd* metal, (d) covalent insulator, and (e) doped covalent insulator.

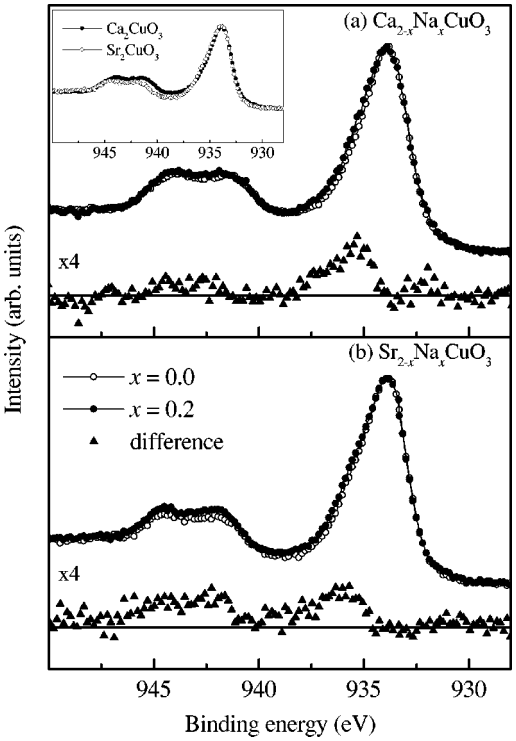

FIG. 5. Cu $2p_{3/2}$ spectra of (a) $Ca_{2-x}Na_xCuO_3$ and (b) $Sr_{2-x}Na_xCuO_3$ for $x=0.0$ (open circles) and 0.2 (solid circles). The triangles shows the expanded difference spectra of the doped compound with respect to the parent one. The inset shows the Cu $2p_{3/2}$ spectra of Sr_2CuO_3 (open circles) and Ca_2CuO_3 (solid circles).

tween the Cu $3d$ and O $2p$ states determines the energy separation [$f(t)$ in the figure] between the bonding and antibonding states. The presence of the oxygen levels above the Cu *d* levels, as observed in the valence-band spectra, indicates a large oxygen $2p$ character of the antibonding states. In the parent compounds, the half filled antibonding level changes to an insulating ground-state configuration due to the electron correlation *U* and finite *t*.

Doping-induced structural changes lead to an increase in $t(=t')$. This enhancement in *t* is expected to increase the separation between the bonding and antibonding states as shown in Fig. 4(b) (doped case) relative to the undoped case [Fig. 4(a)]. It is to be noted here that since the doped holes are localized, as observed in the BI spectra, the local electronic structure will be similar to a band insulating phase with no electron in the antibonding level.

The overall change in the band scheme can be described schematically as shown in the lower panel of Fig. 4. Here, the schemes in Figs. 4(c) and 4(d) demonstrate the cases with the upper Hubbard band within the oxygen $2p$ bandwidth in the absence and presence of *t*. For small *t*, the system will exhibit metallic behavior and is termed a *pd* metal [see Fig. 4(c)]. With increase in *t*, the system becomes insulating for a certain value of *t*. Since, the finite value of *t*, in addition to the electron correlation effects, is the origin of this insulating phase, these systems are termed covalent insulators.[17,18,36] Sr_2CuO_3 and Ca_2CuO_3 exhibit such covalent insulating behavior. Doping of holes to this system introduces an increase in *t* [see Figs. 4(a) and 4(b)] with the doped holes primarily localized at the oxygen sites. Thus, the band scheme will be a sum of the contributions from the doped and undoped sites, as shown in Fig. 4(e).

In Ca_2CuO_3, however, the change in *t* is expected to be less pronounced due to the competing tendencies arising from the larger Na^{1+} ionic radius compared to Ca^{2+} ionic radius ($\sim$1.06 Å) and the increased valency at the Cu sites due to the heterovalent substitution. Thus, we observe no significant change in the spectral positions in Fig. 2. The redistribution of the spectral weight observed in the BI spectra (see Fig. 2) is essentially due to the enhancement in the population of holes at the apical oxygen sites due to doping. The observation of these localized doped holes associated with a local structural distortion supports the interpretation of the charge transport in the doped compounds as primarily driven by the hopping of small polarons.[19]

We now turn to the Cu $2p_{3/2}$ spectra for all the compounds, shown in Fig. 5. The spectra from doped and undoped Ca_2CuO_3 and Sr_2CuO_3 have been overlapped in Figs. 5(a) and 5(b), respectively. The filled circles represent the doped cases and the open ones, the undoped compounds. The

main intense feature around 934-eV binding energy arises from final states with primarily $3d^{10}L$ electronic configuration. Thus, the Cu $2p$ core holes are screened by transferring an electron to the Cu $3d$ level from the ligand levels. Therefore, these are termed well-screened states. The broad feature spread over the energy range of 938–950 eV binding energies is the satellite feature associated with the Cu $2p_{3/2}$ main photoemission signal. Features in this energy region are known to arise from the presence of strong electron-electron interactions and are often termed the poorly screened states, since these are essentially dominated by the $3d^9$ electronic configurations in the final states in the presence of a Cu $2p$ core hole. The intensity of the satellite features relative to the main signal appears to be small due to a small charge transfer energy Δ in these one-dimensional systems.[8,9]

The intensity of the satellite in doped Ca_2CuO_3 remains the same as in the parent compound. However, there is a small increase in the satellite intensity in $Sr_{1.8}Na_{0.2}CuO_3$ compared to Sr_2CuO_3, as can be clearly seen in the difference spectrum represented by the solid triangles in the figure. In order to understand this spectral change, we overlap the Cu $2p_{3/2}$ spectra of Sr_2CuO_3 and Ca_2CuO_3 in the inset of the figure. The spectra exhibit some modifications in satellite intensity and line shape. The detailed analysis[8,9] of these spectra in terms of the cluster and Anderson impurity model calculations attributed these spectral modifications to a small difference in the charge transfer energy of these systems. Thus, the changes due to doping of hole states in Sr_2CuO_3 might be attributed to a small modification of the interaction parameters, specifically the charge-transfer energy in this system.

The main signals are found to be somewhat broader in doped compounds compared to the undoped ones. This can be observed clearly in the difference spectra, shown in the figure. It is well known[37] that the width of the main signal arises essentially due to the different well-screened final states in the photoemission process. The experimental study[37] along with their theoretical analysis[38,39] suggests that the strongest intensity appearing at about 934-eV binding energy is due to the final states $3d^{10}L$ where the ligand hole, L forms a singlet with the neighboring $3d$ hole. These are often termed as Zhang-Rice singlets.[37–40] On the other hand, the shoulder close to 935-eV binding energy (appearing as an asymmetry in the spectra due to the resolution broadening) corresponds to the $3d^{10}L$ final states with the single ligand hole confined within the ligands around the site of core-hole creation. The increase in intensity of this feature with doping indicates more pronounced localization of the holes transferred to the ligand levels within the cluster with the core hole in the final states. It is clear that a detailed theoretical analysis needs to be performed for the doped compounds involving multiple Cu sites in order to obtain a quantitative understanding of the changes in the spectra experimentally observed. However, such calculations need large computational infrastructure far beyond the scope of the present work.

IV. CONCLUSIONS

In summary, we have investigated the electronic structure of doped and undoped one-dimensional cuprates Ca_2CuO_3 and Sr_2CuO_3 by means of photoemission and inverse photoemission spectroscopies. All the spectra suggest the local character of the doped holes in these systems. The changes introduced by doping in the valence- and conduction-band spectra indicates the localization of the doped holes at the oxygen sites. The spectral features appear to be additive in these doped compounds. The unusual spectral modification in the conduction-band spectra suggests a dominant role of the hopping interaction strength related to the change in the local structure of the CuO_4 units in determining the electronic structure rather than the electron-electron interactions that is the dominant factor in most other cases. This study thus, provides the example of the evolution of the spectral functions as a function of doping in a correlated covalent insulator.

ACKNOWLEDGMENTS

The authors thank Professor C.N.R. Rao for continued support, the Department of Science and Technology, Government of India for financial assistance. K.M. thanks the Council of Scientific and Industrial Research, Government of India for financial assistance.

*Present address: Department of Condensed Matter Physics and Materials Science, Tata Institute of Fundamental Research, Homi Bhabha Road, Colaba, Mumbai - 400 005, India.

†Also at Jawaharlal Nehru Center for Advanced Scientific Research, Bangalore. Electronic address: sarma@sscu.iisc.ernet.in

[1] E. Dagotto, Rev. Mod. Phys. **66**, 763 (1994).

[2] D.J. Scalapino, Phys. Rep. **250**, 329 (1995).

[3] H. Suzuura, H. Yasuhara, A. Furusaki, N. Nagaosa, and Y. Tokura, Phys. Rev. Lett. **76**, 2579 (1996).

[4] C. Kim, A.Y. Matsuura, Z.-X. Shen, N. Motoyama, H. Eisaki, S. Uchida, T. Tohyama, and S. Maekawa, Phys. Rev. Lett. **77**, 4054 (1996).

[5] R. Neudert, M. Knupfer, M.S. Golden, J. Fink, W. Stephan, K. Penc, N. Motoyama, H. Eisaki, and S. Uchida, Phys. Rev. Lett. **81**, 657 (1998).

[6] F.D.M. Haldane, Phys. Lett. **93A**, 464 (1983); Phys. Rev. Lett. **50**, 1153 (1983).

[7] N. Motoyama, H. Eisaki, and S. Uchida, Phys. Rev. Lett. **76**, 3212 (1996).

[8] K. Maiti, D.D. Sarma, T. Mizokawa, and A. Fujimori, Europhys. Lett. **37**, 359 (1997).

[9] K. Maiti, D.D. Sarma, T. Mizokawa, and A. Fujimori, Phys. Rev. B **57**, 1572 (1998).

[10] Z. Hiroi, Z. Takano, M. Asuma, and Y. Takeda, Nature (London) **364**, 315 (1993).

[11] Y.J. Shin, E.D. Manova, J.M. Dance, P. Dordor, J.C. Grenier, E. Marquesteut, J.P. Doumere, M. Pouchard, and P. Hagenmuller, Z. Anorg. Allg. Chem. **616**, 201 (1992).

[12] H. Müller-Buschbaum, Angew. Chem. **89**, 704 (1977).

[13] D.R. Lines, M.T. Weller, D.B. Currie, and D.M. Ogbome, Mater. Res. Bull. **26**, 323 (1991).
[14] R.D. Shanon, Acta Crystallogr., Sect. A: Cryst. Phys., Diffr., Theor. Gen. Crystallogr. **A32**, 751 (1976).
[15] Y. Tokura, S. Koshihara, T. Arima, H. Tagaki, S. Ishibashi, T. Ido, and S. Uchida, Phys. Rev. B **41**, 11 657 (1990).
[16] K. Maiti, Priya Mahadevan, and D.D. Sarma, Phys. Rev. B **59**, 12 457 (1999).
[17] D.D. Sarma, H.R. Krishnamurthy, S. Nimkar, S. Ramasesha, P.P. Mitra, and T.V. Ramakrishnan, Pramana, J. Phys. **38**, L531 (1992).
[18] Seva Nimkar, D.D. Sarma, H.R. Krishnamurthy, and S. Ramasesha, Phys. Rev. B **48**, 7355 (1993).
[19] M. Pouchard, Y.J. Shin, J.P. Doumerc, and P. Hagenmuller, Eur. J. Solid State Inorg. Chem. **28**, 461 (1991).
[20] S. Kondoh, K. Fukuda, and M. Sato, Solid State Commun. **65**, 1163 (1988).
[21] H. Eskes, M.B. Meinders, and G.A. Sawatzky, Phys. Rev. Lett. **67**, 1035 (1991).
[22] C.T. Chen, F. Sette, Y. Ma, M.S. Hybertsen, E.B. Stechel, W.M.C. Foulkes, M. Schluter, S-W. Cheong, A.S. Cooper, L.W. Rupp, Jr., B. Batlogg, Y.L. Soo, Z.H. Ming, A. Krol, and Y.H. Kao, Phys. Rev. Lett. **66**, 104 (1991).
[23] S.L. Cooper, G.A. Thomas, J. Orenstein, D.H. Rapkine, A.J. Millis, S.-W. Cheong, A.S. Cooper, and Z. Fisk, Phys. Rev. B **41**, 11 605 (1990).
[24] K. Maiti and D.D. Sarma (unpublished).
[25] R. Neudert, M.S. Golden, M. Knupfer, S. Haffner, J. Fink, S.-L. Drechsler, J. Málek, H. Rosener, R. Hayn, K. Ruck, G. Krabbes, W. Stephan, K. Penc, V.Y. Yushankhai, C. Waidacher, J. Richter, K.W. Becker, T. Osafune, N. Motoyama, H. Eisaki, and S. Uchida, Physica C **317-318**, 312 (1999).
[26] K. Maiti, Ph.D thesis, Indian Institute of Science, Bangalore, India, 1998.
[27] Y.J. Shin, E.D. Manova, J.M. Dance, P. Dordor, J.C. Grenier, E. Marquesteut, J.P. Doumere, M. Pouchard, and P. Hagenmuller, Z. Anorg. Allg. Chem. **616**, 201 (1992).
[28] K. Maiti and D.D. Sarma, Phys. Rev. B **58**, 9746 (1998).
[29] E. Pellegrin, J. Jaanen, H.-J. Lin, G. Meigs, C.T. Chen, G.H. Ho, H. Eisaki, and S. Uchida, Phys. Rev. B **53**, 10 667 (1996).
[30] G. Kotliar and G. Moeller, in *Spectroscopy of Mott Insulators and Correlated Metals*, edited by A. Fujimori and Y. Tokura (Springer-Verlag, Berlin, 1994), p. 15.
[31] J.J. Yeh and I. Lindau, At. Data Nucl. Data Tables **32**, 1 (1985).
[32] D.D. Sarma, A. Chainani, S.R. Krishnakumar, E. Vescovo, C. Carbone, W. Eberhardt, O. Rader, Ch. Jung, Ch. Hellwig, W. Gudat, H. Srikanth, and A.K. Raychaudhuri, Phys. Rev. Lett. **80**, 4004 (1998).
[33] D. D. Sarma, S.R. Barman, H. Kajueter, and G. Kotliar, Europhys. Lett. **36**, 307 (1996).
[34] D.D. Sarma, S.R. Barman, H. Kajueter, and G. Kotliar, Physica B **223-224**, 496 (1996).
[35] H. Kajueter, G. Kotliar, D.D. Sarma, and S.R. Barman, Int. J. Mod. Phys. B **11**, 3849 (1997).
[36] D.D. Sarma, J. Solid State Chem. **88**, 45 (1990).
[37] T. Böske, K. Maiti, O. Knauff, K. Ruck, M.S. Golden, G. Krabbes, and J. Fink, Phys. Rev. B **57**, 138 (1998).
[38] K. Okada, A. Kotani, K. Maiti, and D.D. Sarma, J. Phys. Soc. Jpn. **65**, 1844 (1996).
[39] M.A. van Veenendaal, H. Eskes, and G.A. Sawatzky, Phys. Rev. B **47**, 11 462 (1993).
[40] F.C. Zhang and T.M. Rice, Phys. Rev. B **37**, 3759 (1988).